

On the P-Coordinating Limit of NHC–Phosphenium Cations toward Rh^I Centers**Carine Maaliki,^[a, b] Christine Lepetit,^[a, b] Yves Canac,^{*,[a, b]} Christian Bijani,^[a, b]
Carine Duhayon,^[a, b] and Remi Chauvin^{*,[a, b]}

Abstract: Two types of imidazoliophosphane with additional electron-withdrawing substituents, such as alkoxy or imidazolio groups, are experimentally described and theoretically studied. Diethyl *N,N'*-2,4,6-methyl(phenyl)imidazoliophosphonite is shown to retain a P-coordinating ability toward a {RhCl(cod)} (cod = cycloocta-1,5-diene) center, thus competing with the cleavage of the labile C–P bond. Derivatives of *N,N'*-phenylene-bridged diimidazolylphenylphosphane were isolated in good yield. Whereas the dicationic phosphane proved to be inert in the presence of [{RhCl(cod)}₂], the monocationic counterpart was shown to retain the P-coordinating ability toward a {RhCl(cod)} center, thus competing with the N-coordinating ability of the nonmethylated imidazolyl sub-

stituent. The ethyl phosphinite version of the dication, thus possessing an extremely electron-poor P^{III} center, was also characterized. According to the difference between the calculated homolytic and heterolytic dissociation energies, the N₂C…P bond of imidazoliophosphanes with aryl, amino, or alkoxy substituents on the P atom is shown to be of dative nature. The P-coordinating properties of imidazoliophosphanes with various combinations of phenyl or ethoxy substituents on the P atom and those of six diimidazolophosphane derivatives with zero, one, or two methyl-

ium substituents on the N atom, were analyzed by comparison of the corresponding HOMOs and LUMOs and by calculation of the IR C=O stretching frequencies of their [RhCl(CO)₂] complexes. Comparison of the ν_{CO} values allows the family of the electron-poor Im⁺PRR' (Im = imidazolyl) potential ligands to be ranked in the following order versus (R,R'): P(OEt)₃ < (Ph,Ph) < (Ph,OEt) < (OEt,OEt) < PF₃ < (Ph,Im) < (Ph,Im⁺) < (OEt,Im⁺). The (Ph,Im) representative is therefore the least electron-donating phosphane for which coordinating behavior toward a Rh^I center has been experimentally evidenced to date. Ultimate applications in catalysis could be envisaged.

Keywords: carbene ligands • dative bonds • donor–acceptor systems • heterocycles • phosphane ligands • rhodium

Introduction

Beyond the vertical periodicity based on the similarity of the valence-electron shell, thus making phosphorus the nitrogen “analogue”, diagonal periodicity, based on the similarity of electronegativity,^[1] has also been invoked for making phosphorus the carbon “copy”.^[2] The diagonal analogy becomes particularly relevant in terms of reactivity for low-coordinate phosphorus and carbon compounds.^[3] This

proposition is illustrated by the isolobal analogy between phosphenium ions R₂P⁺ and carbenes R₂C: in the singlet spin state,^[4] which are both prone to be stabilized by coordination with either a Lewis acid (LA) or a Lewis base (LB). In amidiniophosphanes,^[5] which constitute a particular class of carbeniophosphanes represented by a R₂N₂⁺C–PR'₂ Lewis structure, the carbon and phosphorus centers were shown to preserve their Lewis acido–basic characters, and thus their common ambiphilic chemical nature in a complementary manner for LA = R₂P⁺ and LB = R₂C: The strict donor–acceptor character of a given X–Y bond is indeed not formal:^[6] it is determined by the energetic preference for a heterolytic dissociation mode over the homolytic mode. The dative nature of the R₂N₂C→PR'₂⁺ bond was thus early suggested^[7] and recently demonstrated both experimentally and theoretically.^[8] The Lewis base character of the phosphenium Lewis acid was also shown to persist in the adduct by coordination of Ph₂P⁺ motifs to Lewis acidic transition-metal centers (Rh^I, Pd^{II}),^[5] thus giving rise to carbon–phosphorus–metal ternary complexes.^[8c] A natural question addresses the limit of the coordinating ability of the R₂P⁺ lone pair of electrons versus the electron-withdrawing character of the R substituents. Upon substitution

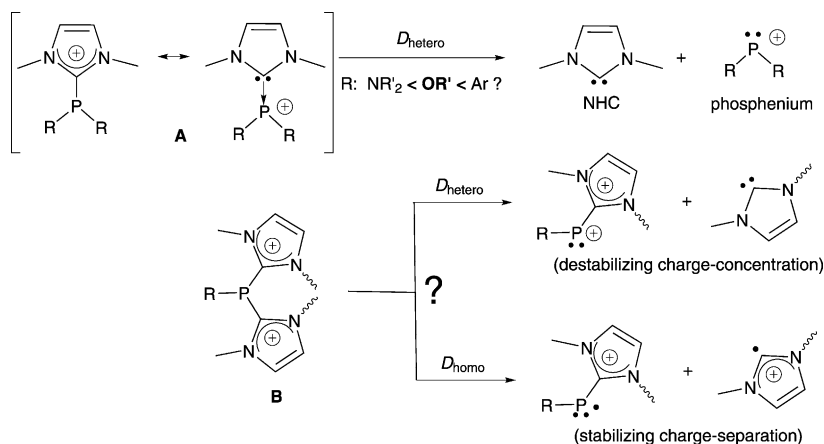
[a] C. Maaliki, Dr. C. Lepetit, Dr. Y. Canac, Dr. C. Bijani, C. Duhayon, Prof. R. Chauvin
Laboratoire de Chimie de Coordination (LCC), CNRS
205, Route de Narbonne, 31077 Toulouse (France)
Fax: (+33) 561-553-003
E-mail: yves.canac@lcc-toulouse.fr
chauvin@lcc-toulouse.fr

[b] C. Maaliki, Dr. C. Lepetit, Dr. Y. Canac, Dr. C. Bijani, C. Duhayon, Prof. R. Chauvin
Université de Toulouse
UPS, INP; LCC
31077 Toulouse (France)

[**] NHC = N-heterocyclic carbene.

Supporting information for this article is available on the WWW under <http://dx.doi.org/10.1002/chem.201104046>.

at the P atom by electron-withdrawing groups, weakening of the intrinsic coordinating ability of the P^+ lone pair of electrons on a free phosphonium ion is accompanied by strengthening of the $NHC \rightarrow P^+$ bond ($NHC = N$ -heterocyclic carbene). Conversely, indeed, free R_2P^+ phosphonium ions are stabilized by π -electron-donating R substituents, such as amino groups, in the same way, and to a similar extent, as in stable diaminocarbenes,^[9] with concomitant destabilization of the $NHC \rightarrow P(NR'_2)_2^+$ bond. A NHC -diaminophosphonium adduct was however reported by Baker and co-workers^[10] who showed that the addition of an electron-rich platinum(0) complex (i.e., $[Pt(PPh_3)_3]$) resulted in the instantaneous cleavage of the anyway labile C–P bond, likely via a NHC -diaminophosphonium/platinum complex (which was however neither isolated nor spectroscopically detected). Complementary to the case of the aryl and amino R substituents is the case for the oxy R substituents. Whereas the π -donating character (+M effect) of oxygen atoms is weaker than that of nitrogen atoms, the σ -withdrawing character (–I effect) varies in the opposite sense: the overall effect on the stability of the corresponding free phosphonium ions has to be compared with that of aryl substituents. Inversion of the periodicity can be anticipated (both diaryl- and dioxyphosphonium ions are expected to be less stable than the diaminophosphonium paradigms), but the P-donating character of NHC -dioxyphosphonium adducts **A** remains an open issue (Scheme 1).



Scheme 1. Possible dissociation modes of imidazoliophosphanes **A** (top) and diimidazoliophosphanes **B** (bottom).

More electron-withdrawing than alkoxy substituents are cationic amidino substituents, in which the positive charge is π -conjugated to the P^{III} center (in most reported cationic phosphanes, the positive charge is indeed conjugatively insulated in a remote position from the P center).^[11] Although the stability of poly(amidino)-phosphanes has been illustrated

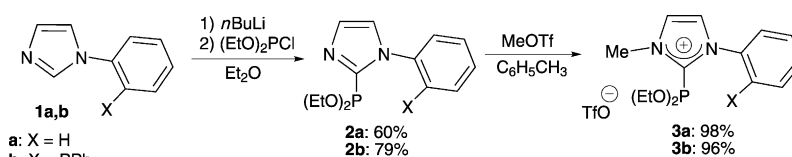
both in the diimidazolium series (adducts of type **B**)^[12] and in the cross-vinylous tris(diamino)cyclopropenium series,^[13] the dative nature of the N_2^+C-P bonds is not a priori guaranteed; the homolytic dissociation mode could, indeed, be favored by the corresponding electrostatic relaxation (Scheme 1).^[6] Although the coordinating ability of tris(diamino)cyclopropeniphosphanes toward the anionic trichloropalladate center has been reported, the electrostatic driving force is certainly the determining factor.^[13] On the other hand, the coordinating ability of diimidazoliophosphanes toward neutral metallic centers remains unknown, and thus deserves investigation from a fundamental viewpoint, keeping mind the possibility of applications in catalysis. In the following, the intrinsic stability and coordination chemistry of imidazoliophosphanes of type **A** and **B** are studied by using experimental and theoretical investigation tools. The results will be discussed on the basis of the electronic and electrostatic features of the systems.

Results and Discussion

Experimental results

Systems of type A: Amidiniophosphonites (R = alkoxy; Scheme 1):

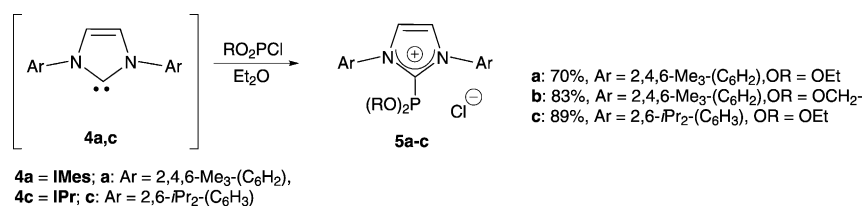
Two complementary approaches were envisaged to access the amidiniophosphonites. The first approach starts from the readily available 1-(1-phenyl)-1*H*-imidazole **1a** or 1-(2-diphenylphosphino)-1*H*-imidazole **1b**.^[14] Subsequent addition of one equivalent of *n*BuLi in Et_2O and a stoichiometric amount of chlorodiethylphosphite allowed phosphonite **2a** and phosphane–phosphonite **2b** to be obtained in 60 and 79% yield, respectively (Scheme 2). Finally, a single equivalent of methyl triflate (MeOTf) reacted selectively with **2a** and **2b** in toluene to give the targeted amidiniophosphonites **3a** and **3b** in quasi-quantitative yields. The ^{31}P NMR chemical shift of **3a** ($\delta_p = +142.4$ ppm) is in the typical range for phosphonite compounds.^[15] Whereas the ^{31}P NMR resonance of the phosphonite fragment of **3b** is



Scheme 2. Synthesis of the amidiniophosphonites **3a** and **3b** from the imidazole precursors **1a** and **1b**.

observed in the same range ($\delta_p = +141.1$ ppm, doublet, $J_{PP} = 65.8$ Hz), the second resonance ($\delta_p = -17.4$ ppm, doublet, $J_{PP} = 65.8$ Hz) is in good agreement with the triarylphosphane fragment. The ionic nature of the products was indicated by a very low solubility in nonpolar solvents and by a deshielded ^1H NMR signal that corresponds to the *N*-methyl substituent ($\delta_H = +4.1$ ppm; Scheme 2).

The alternative strategy consists of the generation of the free NHCs **4a** and **4c** (with IMes and IPr substituents, respectively; Scheme 3) from the corresponding imidazolium

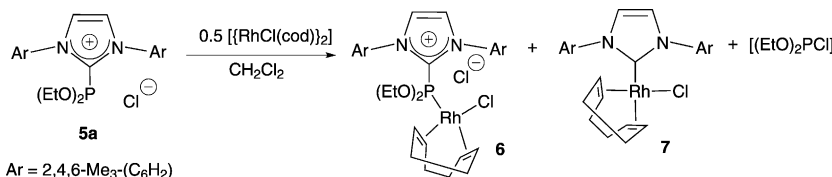


Scheme 3. Preparation of the amidiniophosphonites **5a–5c** from the free NHCs **4a–4c** generated in situ.

salts by addition of a suitable base.^[16] Subsequent addition of one equivalent of chlorodiethylphosphite in Et₂O afforded the cationic phosphonites **5a** and **5c** in 70 and 89% yield, respectively (Scheme 3). The ^{31}P NMR spectrum of the products confirmed the formation of the imidazoliophosphane moieties (**5a**: $\delta_p = +149.9$ ppm; **5c**: $\delta_p = +156.6$ ppm). The addition of IMes **4c** to 2-chloro-1,3-dioxaphospholane gave amidiniophosphonite **5b** in 83% yield. In comparison to **5a**, the more-shielded ^{31}P NMR signal of **5b** ($\delta_p = +134.6$ ppm) was attributed to the presence of a five-membered cyclic phosphonite. Although the amidiniophosphonites appeared to be stable whatever the anion (**3a,b**: TfO[−]; **5a–c**: Cl[−]), they decomposed over time in solution ($t_{1/2} \approx 10$ – 20 h at 20 °C in CH₂Cl₂), thus releasing the corresponding imidazolium salt and primary phosphane oxide by hydrolytic cleavage of the N₂⁺C–P bond.^[18]

The amidiniophosphonite **5a** was treated with 0.5 equivalents of $[\{\text{RhCl}(\text{cod})\}_2]$ (cod = cycloocta-1,5-diene) in CH₂Cl₂. The ^{31}P NMR spectrum of the reaction mixture displayed a doublet signal at high field, thus revealing the coordination of the P atom to the Rh center ($\delta_p = +121.2$ ppm, doublet, $^1J_{\text{PRh}} = 241.0$ Hz). The formation of complex **6** shows that in spite of the presence of two electron-withdrawing ethoxy substituents at the P atom, phosphonite **5a** retains some donor character toward a moderately Lewis acidic Rh^I center (Scheme 4).

The phosphonite/rhodium complex **6** was however obtained in poor yield (7%), along with the NHC/rhodium complex **7** (24%) and the starting imidazolium salt IMes·HCl (69%). The formation of **7** can be explained by displacement of the NHC moiety from the P



Scheme 4. Preparation of the rhodium(I) complex **6** of the amidiniophosphonite ligand **5a** accompanied by cleavage of the P–C bond.

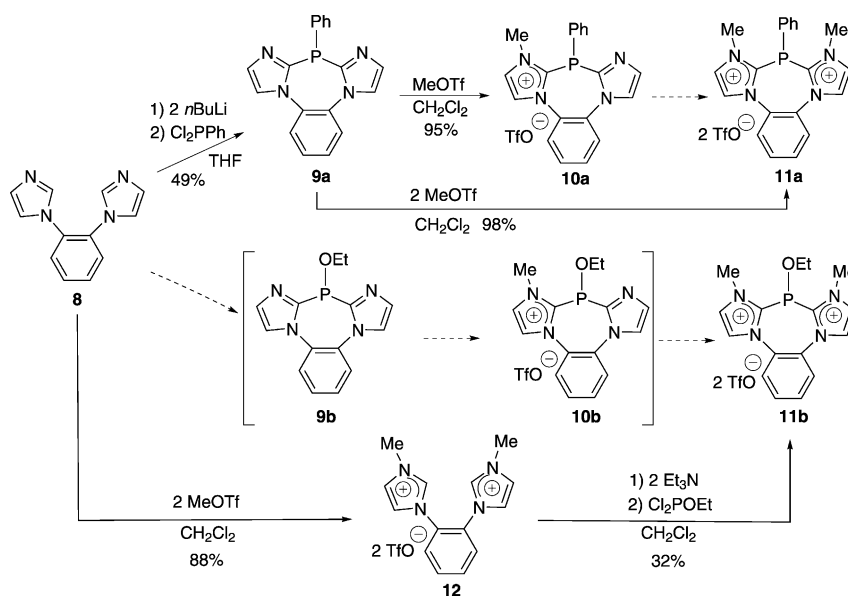
atom to the Rh atom, thus confirming the weakness, and perhaps the dative nature, of the N₂⁺C–P bond, as observed for the free ligand. It has been recently reported that a relatively weak nucleophile, such as the chloride ion, induced the heterolytic cleavage of imidazoliophosphanes to the chlorodiphenylphosphane and corresponding NHC moieties at 50 °C.^[8] The same cleavage was also observed in the coordination sphere of a Pd complex, with subsequent trapping of the NHC moiety by the Pd^{II} center.^[8] A similar reactivity, albeit at lower temperature, is thus observed for imidazoliophosphonite analogues.

Systems of type B: diamidiniophosphanes (R = aryl, alkoxy; Scheme 1):

The preparation of diamidiniophosphanes started from the readily available 1,2-di(*N*-imidazolyl)benzene **8**.^[17] Double deprotonation of **8** with two equivalents of *n*BuLi in THF followed by addition of one equivalent of dichlorophen-

ylphosphane afforded the cyclic diimidazolophosphane **9a** in 49% yield (Scheme 5). The $^{31}\text{P}\{^1\text{H}\}$ NMR spectrum of **9a** displayed a singlet signal at very high field ($\delta_p = -60.8$ ppm), consistent with a tris-annulated cyclic environment of the P^{III} atom. The exact structure of **9a** was confirmed by X-ray diffraction analysis of colorless crystals deposited from a CH₂Cl₂/Et₂O mixture (Figure 1).^[18]

The addition of two equivalents of MeOTf to the neutral diimidazolophosphane **9a** in CH₂Cl₂ afforded the dicationic diimidazolophosphane **11a** in 98% yield. The use of one equivalent of MeOTf allowed the monocationic imidazoliophosphane **10a** to be isolated in 95% yield (Scheme 5). Both products were fully characterized by multinuclear NMR spectroscopy, and in particular by using $^{31}\text{P}\{^1\text{H}\}$ NMR spectroscopic analysis (**10a**: $\delta_p = -68.5$ ppm (singlet); **11a**: $\delta_p = -76.2$ ppm (singlet)). The successive methylation steps in the series **9a**→**10a**→**11a** resulted in a shielding of approximately $\Delta\delta = 8$ ppm each in the ^{31}P NMR spectra. The structure of dication **11a** was finally confirmed by X-ray diffraction analysis of single crystals obtained from a MeCN/Et₂O mixture (Figure 1).^[18] In both cases (i.e., **9a** and **11a**), the seven-membered phosphoracycle is boat-shaped, the prow occupied by the P atom and the stern by the C–C bond of the phenylene bridge. Although the conformation is mainly dictated by steric constraints, an



Scheme 5. The principle of the preparation of the diimidazolophosphane derivatives **9**–**11** from 1,2-diimidazolylbenzene (**8**) through either successive *N*-methylation of the intermediate **9a** in the phosphane series **a** or via the elusive bis(diaminocarbene) of the diimidazolium salt **12** in the phosphinite series **b** (route **a** via the putative phosphinites **9b** and **10b** was not attempted).

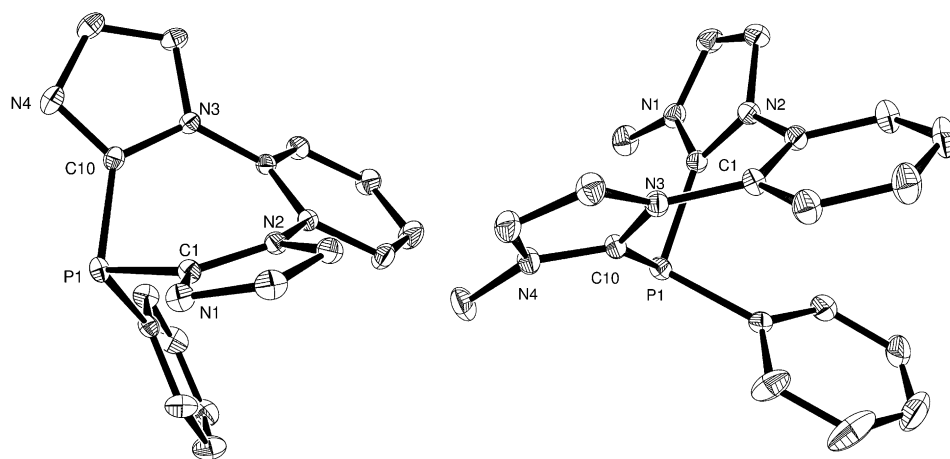


Figure 1. ORTEP views of the X-ray crystal structures of neutral and dicationic phosphanes **9a** (left) and **11a** (right). The thermal ellipsoids are drawn at the 30% probability level (the triflate anions and H atoms are omitted for clarity). Selected bond lengths [Å] and angles [°] of **9a**: C1–P1 1.8084(12), C10–P1 1.8078(12), N1–C1 1.3229(16), N2–C1 1.3818(14); C1–P1–C10 95.75(5), N1–C1–N2 111.00(10), N2–C1–P1 125.50(9); and **11a**: C1–P1 1.818(3), C10–P1 1.822(3), N1–C1 1.339(3), N2–C1 1.352(4); C1–P1–C10 92.61(12), N1–C1–N2 106.7(2), N2–C1–P1 128.0(2).

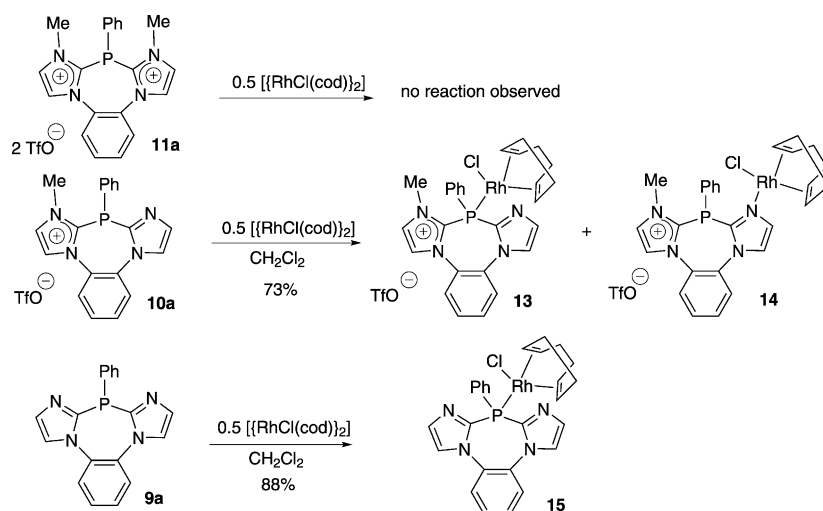
auxiliary driving force is π -stacking of the *P*-phenyl substituent with the phenylene bridge. From the neutral phosphane **9a** to the dimethylated version **11a**, no significant differences concerning the bond lengths and angle values were observed.

Ethyl diimidazolophosphinite **11b** was targeted as a “poorer analogue” of imidazolophosphane **11a** (Scheme 5). Its preparation was attempted by alkylation of the *sp*² N atoms of the imidazole fragments prior to the phosphan-diylation step. The dication **12** was obtained by di-

methylation of 1,2-diimidazolylbenzene **8**.^[14b] Subsequent addition of one equivalent of dichloro(ethyl)phosphite in the presence of two equivalents of Et₃N afforded diamidiniophosphinite **11b** in 32% yield. As expected, the unique ³¹P NMR signal of **11b** is more deshielded ($\delta_p = +31.4$ ppm) than that of the related diamidiniophosphane **11a** ($\delta_p = -76.2$ ppm) and more shielded than those of acyclic imidazoliophosphonites **3a,b** ($\delta_p \approx 141$ – 142 ppm).

The potential ligands **9a**, **10a**, and **11a** were investigated by cyclic voltammetry, and each of them exhibited a single irreversible oxidation peak at the following potentials versus the saturated calomel electrode (SCE): $E_p^{ox} = +1.02$, $+2.28$, and $+2.83$ V for **9a**, **10a**, and **11a**, respectively. These data confirm the increasing electron deficiency of the oxidation site (likely the PPh group) in the series **9a** \rightarrow **10a** \rightarrow **11a**. As the oxidation potential of phosphanes is recognized as a measure of the electronic endowment of the P atom, coordination of diimidazolophosphane **11a** to a Lewis acid center is, henceforth, anticipated to be a difficult challenge. Whatever the conditions used (solvent, temperature, stoichiometry, and so forth), the treatment of **11a** with $[\{\text{RhCl}(\text{cod})\}_2]$ did not lead to any coordination and the starting dication was recovered, as indicated by multinuclear NMR spectroscopic analysis. Attempts at treating **11a** with other Lewis acids ($[\text{PdCl}_2(\text{PhCN})_2]$, CuI, CuBr₂, BH₃) or oxidizing agents (S₈, H₂O₂) were unsuccessful as well. These results indicate that the electron deficiency of **11a**, and all the more of **11b**, is beyond the coordinating limit to any neutral Lewis acid.

Nevertheless, the monocationic imidazo-imidazoliophosphane **10a** reacted with a slight excess of $[\{\text{RhCl}(\text{cod})\}_2]$ in CH₂Cl₂. After 24 hours at 40 °C, the ³¹P NMR spectrum of the mixture and other analyses indicated that complexes **13** and **14** were formed in a 1:1 ratio and 73% overall yield. The ³¹P{¹H} NMR resonance of **13** at $\delta_p = +15.8$ ppm (dou-



Scheme 6. The outcome of the addition of the $[\{\text{RhCl}(\text{cod})\}_2]$ complex to the phenylphosphanes **9a–11a**.

blet, $J_{\text{PRh}} = 166.1$ Hz) is in agreement with the coordination of the lone pair of electrons on the P atom to a Rh^{I} center (Scheme 6). In contrast, the $^{31}\text{P}\{^1\text{H}\}$ NMR singlet signal of **14** (at $\delta_{\text{p}} = -69.1$ ppm) is similar to that of **10a**, thus ruling out any direct $\text{P}\cdots\text{Rh}$ interaction. The exact structure was finally determined by X-ray diffraction analysis of single yellow crystals of **14** deposited from CH_2Cl_2 (see Scheme 6 and Figure 2).^[18]

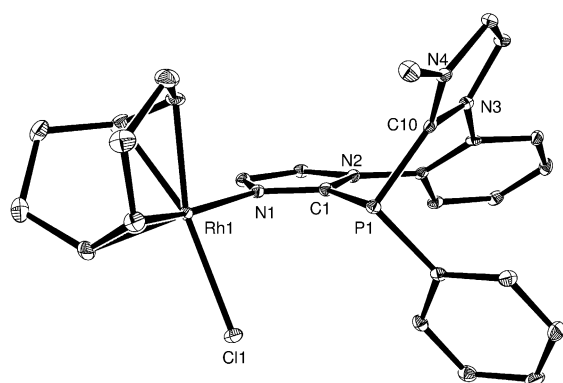


Figure 2. ORTEP view of the X-ray crystal structure of rhodium complex **14**. The thermal ellipsoids are drawn at the 30% probability level (the triflate anions and H atoms are omitted for clarity). Selected bond lengths [Å] and angles [°]: C1–P1 1.8120(17), C10–P1 1.8234(18), N1–C1 1.325(2), N2–C1 1.365(2), N1–Rh1 2.0944(14), Rh1–Cl1 2.3905(4); C1–P1–C10 94.78(7), N1–C1–N2 110.09(14), N2–C1–P1 128.20(13).

The structure of **14** evidences the coordination of a sp^2 N atom to a Rh^{I} atom located at the center of a quasi-square-planar environment. The lone pair of electrons on the P atom is directed toward the metallic center at a $\text{P}\cdots\text{Rh}$ distance of approximately 3.43 Å, which is much greater than the sum of the corresponding covalent radii (≈ 2.31 Å), but smaller than the sum of corresponding van der Waals radii (≈ 3.8 Å). This outcome suggests the existence of a residual

interaction between the P and Rh atoms. As observed for phosphanes **9a** and **11a**, the P atom is strongly pyramidalized (sum of the angles: 300.2, 295.5, and 295.2°, for **9a**, **11a**, and **14**, respectively), with the phenyl substituent on the P atom located on the same side as the *ortho*-phenylene bridge.

The P-coordinated rhodium complex **13** thus indicates that the lone pair of electrons on the P atom of the monocationic phosphane **10a** retains sufficient donating character. Nevertheless, the concomitant formation of the N-coordinated rhodium complex **14** suggests that the monocationic phosphane

10a is “on the good side” of the P-coordination limit with a neutral Rh^{I} center.

To confirm the latter hypothesis, neutral phosphane **9a** was treated with $[\{\text{RhCl}(\text{cod})\}_2]$ in CH_2Cl_2 . A reaction was observed to occur readily at room temperature, thus affording rhodium complex **15** in 88% yield. The doublet $^{31}\text{P}\{^1\text{H}\}$ NMR signal at $\delta_{\text{p}} = +7.7$ ppm ($J_{\text{PRh}} = 160.0$ Hz) gave clear evidence that the P atom of **15** is directly connected to the Rh^{I} center (Scheme 6). Finally, the exact structure was confirmed by X-ray diffraction analysis of yellow crystals of **15** deposited from a $\text{CH}_2\text{Cl}_2/\text{Et}_2\text{O}$ mixture (Figure 3).^[18] No N-coordinated rhodium complex was detected, thus confirming the stronger P-donating character of phosphane **9a** relative to **10a**.

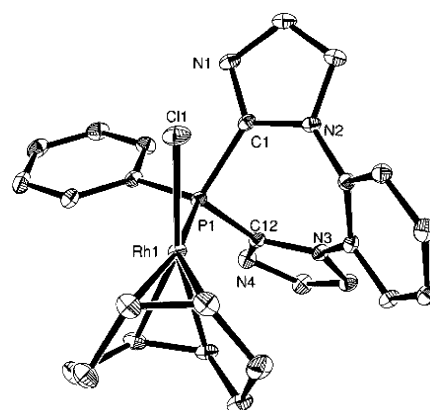


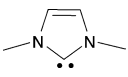
Figure 3. ORTEP view of the X-ray crystal structure of the rhodium complex **15**. The thermal ellipsoids are drawn at the 30% probability level (the H atoms are omitted for clarity). Selected bond lengths [Å] and angles [°]: C1–P1 1.815(3), C12–P1 1.819(3), N1–C1 1.316(3), N2–C1 1.376(3), P1–Rh1 2.2854(6), Rh1–Cl1 2.3636(6); C1–P1–C12 95.80(11), N1–C1–N2 111.9(2), N2–C1–P1 119.02(17).

Theoretical studies

The electron-donating properties of imidazoliophosphanes of type **A** and diimidazoliophosphanes of type **B** (Scheme 1) and the nature of the corresponding N_2C^+-P bonds were investigated by DFT calculations.

Imidazoliophosphanes of type A: *Characterization of the dative N_2C-P bond of imidazoliophosphane models:* On the basis of experimental and theoretical results, imidazoliophosphanes were recently demonstrated to be NHC-phosphenium adducts involving a “true” dative $N_2C \rightarrow PR^1R^2+$ bond (“true” is understood to be according to a quantitative criterion).^[8a] More generally, the degree of dative character of generic $X \cdots P$ bonds varies from the purely covalent case ($X-P$) to the purely ionic case ($X^- \cdots P^+$) depending on the difference in energy between the homolytic (to $X^\cdot + P^\cdot$) and heterolytic (to $X^- + P^+$) dissociation modes.^[6] This character is addressed below in a systematic manner by computation of the corresponding Gibbs dissociation energies $\Delta(\Delta G)$ at 298.15 K in the acetonitrile continuum dielectric medium (polarizable continuum model (PCM) method) at the B3PW91/6-31G** level (Table 1).

Table 1. Quantitative variation of the dative character of C–P bonds over a representative series of neutral, cationic, and dicationic “donor–acceptor adducts”.

Overall charge	Donor	Acceptor	$\Delta G_{\text{homo}}^{[a]}$ [kcal mol ⁻¹]	$\Delta G_{\text{hetero}}^{[b]}$ [kcal mol ⁻¹]	$\Delta(\Delta G)^{[c]}$ [kcal mol ⁻¹]
0	Ph ⁻	⁺ PPh ₂	57.2	112.5	-55.3
	Cl ⁻	⁺ PPh ₂	60.9	34.7	26.2
	H ₃ N	BH ₃	133.5	27.1	106.4 + 1
+1		⁺ PCl ₂	58.6	79.4	-20.8
		⁺ PPh ₂	65.8	57.4	8.4
		⁺ PPh(OH)	66.3	50.6	15.7
		⁺ P(O)Ph ₂	71.1	55.0	16.1
		⁺ P(OMe) ₂	70.5	45.6	24.9
		⁺ P(OEt) ₂	72.2	44.4	27.8
	⁺ P(NMe ₂) ₂	67.6	25.3	42.3 + 2	
+2	NHC	²⁺ P(NHC)Ph	52.6	66.3	-13.7

[a] Homolytic Gibbs dissociation energy at 298.15 K. [b] Heterolytic Gibbs dissociation energy at 298.15 K. [c] $\Delta(\Delta G) = \Delta G_{\text{homo}} - \Delta G_{\text{hetero}}$. The PCM-(U)B3PW91/6-31G** level of calculation in the acetonitrile continuum ($\epsilon = 35.688$) was used. The values for C–P bonds with a dominant covalent character are in bold.

For neutral systems, due to the absence of opposite charge separation,^[6] heterolytic dissociation to neutral closed-shell systems is strongly favored, which is the case for the amine–borane adduct $H_3N \rightarrow BH_3$ ($\Delta(\Delta G) = +106.4$ kcal mol⁻¹). For neutral systems in which heterolytic dissociation to closed-shell species entails a separation of opposite charges, the resulting electrostatic cost generally makes the homolytic dissociation mode to radical species more favored (e.g., by $\Delta(\Delta G) = -55.3$ kcal mol⁻¹ for Ph–PPh₂). Nevertheless, the relative electronegativity of the charged closed-shell moieties may reverse the trend and make the heterolytic

dissociation mode preferred, at least in the polar acetonitrile medium (e.g., by $\Delta(\Delta G) = +26.2$ kcal mol⁻¹ for Cl–PPh₂).

For monocationic NHC–phosphenium systems ($X^\cdot = \text{NHC} = 1,3\text{-bis(methyl)imidazol-2-ylidene}$), the $\Delta(\Delta G)$ values range from -20.8 to 42.3 kcal mol⁻¹ in the following order: $^+PCl_2 < ^+PPh_2 < ^+PPh(OH) < ^+P(O)Ph_2 < ^+P(OR)_2 < ^+P(NMe_2)_2$. Thus, the more stable the phosphenium cation, the greater the $\Delta(\Delta G)$ value, namely, the dative character of the C–P bond (approaching the neutral $H_3N \rightarrow BH_3$ paradigm). Indeed, whereas the homolytic dissociation energy does not vary much over the series ($\Delta G_{\text{homo}} = (65 \pm 7)$ kcal mol⁻¹), the heterolytic counterpart is the main variation factor, which ranges from $\Delta G_{\text{hetero}} = 25.3$ kcal mol⁻¹ for the most stable phosphenium ($^+P(NMe_2)_2$) to $\Delta G_{\text{hetero}} = 79.4$ kcal mol⁻¹ for the least stable one ($^+PCl_2$).

For the dicationic diamino-phosphane [(NHC)₂PPh]²⁺ (an acyclic model of **11a**; Scheme 5), a preference for the homolytic mode ($\Delta(\Delta G) = -13.7$ kcal mol⁻¹) is restored due to the electrostatic strain in the released [(NHC)PPh]²⁺ moiety that results from a heterolytic dissociation. This feature is discussed in detail below.

Electron-donating properties of imidazoliophosphane models: The near-frontier molecular orbitals (FMOs) of ligands of type **A** were investigated in the representative series $[\text{NHC}-\text{PR}^1\text{R}^2]^+$ ($R^i = \text{Ph}$ or OEt , $i = 1, 2$; Figure 4). Upon replacement of a phenyl substituent by an ethoxy substituent, both the HOMO (strongly polarized at the lone pair of electrons on the P atom) and the LUMO (which results from the overlap of the antibonding π^* orbital of the NHC fragment with the p orbital of the original sp² phosphenium fragment) are shifted deeper in energy. The P^{III} atom of imidazoliophosphonites ($R^1 = R^2 = \text{OEt}$) is therefore expected to be less σ -donating and more π -accepting, and

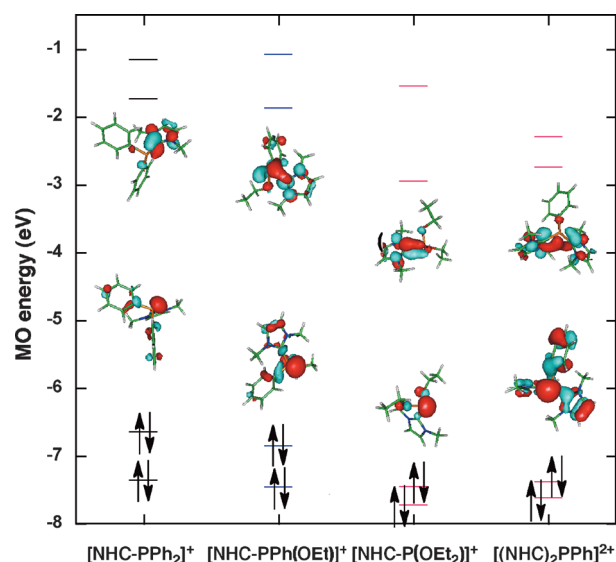


Figure 4. Near-frontier molecular orbitals of representative $[\text{NHC}-\text{PR}^1\text{R}^2]^+$ adducts ($R^i = \text{Ph}$ or OEt , $i = 1, 2$). PCM-B3PW91/6-31G** level of calculation in the acetonitrile continuum ($\epsilon = 35.688$).

thus to be globally a weaker donor toward transition-metal centers, than the P^{III} atoms of imidazoliophosphinites ($R^1 = \text{Ph}$, $R^2 = \text{OEt}$) and imidazoliophosphanes ($R^1 = R^2 = \text{Ph}$). The actual donating character of these ligands was estimated by the average of the calculated IR C=O stretching frequencies in their corresponding $[(\text{NHC}-\text{PR}^1\text{R}^2)\text{Rh}(\text{CO})_2\text{Cl}]^+$ complexes (Table 2). The corresponding $\bar{\nu}_{\text{CO}}$ values were

Table 2. Quantification of the overall donating character of representative ligands L by the average $\bar{\nu}_{\text{CO}}$ values of the two IR C=O stretching frequencies in $[\text{RhLCl}(\text{CO})_2]$ complexes.^[a]

L		$\bar{\nu}_{\text{CO}}$ [cm^{-1}] ^[a]
	$R^1 = R^2 = \text{Ph}$	2071.6
$[\text{NHC}-\text{PR}^1\text{R}^2]^+$	$R^1 = \text{Ph}$; $R^2 = \text{OEt}$	2072.7
	$R^1 = R^2 = \text{OEt}$	2075.9
PF_3		2077.9
$(2,6\text{-Me}_2\text{C}_6\text{H}_3\text{CH}_2\text{CH}_2)\text{PrBu}_2$		2034.9 (2042.5) ^[b]

[a] Calculated at the PBEPBE/6-31G**/LANL2DZ*(Rh) level. [b] Experimentally obtained from reference [21].

indeed widely used to scale the donor properties of phosphanes and NHCs either experimentally or computationally (i.e., the larger the $\bar{\nu}_{\text{CO}}$ value, the weaker the donation).^[19] The PBEPBE/6-31G**/LANL2DZ*(Rh) calculation level was selected for its ability to reproduce the experimental $\bar{\nu}_{\text{CO}}$ measurements (Table 2). In the present series, the large calculated $\bar{\nu}_{\text{CO}}$ values, which range from $\bar{\nu}_{\text{CO}} = 2071.6$ to 2075.9 cm^{-1} for $R^1 = R^2 = \text{Ph}$ and OEt , respectively, are indicative of a weak donating character analogous to the one of PF_3 ($\bar{\nu}_{\text{CO}} = 2077.9 \text{ cm}^{-1}$).^[20] In agreement with the above FMO analysis (Figure 4), replacement of phenyl groups of $\text{NHC} \rightarrow \text{PPh}_2^+$ by ethoxy substituents induces a weakening of the net donating character of the P atom.

Diamidiniophosphanes of type B: *Characterization of the $\text{N}_2\text{C}-\text{P}$ bond of diamidiniophosphanes.* The nature of the $\text{N}_2\text{C}-\text{P}$ bond of diamidiniophosphane **11a** (Scheme 5) was investigated using the model $[\text{NHC}-\text{P}(\text{NHC})\text{Ph}]^{2+}$ ion. In a valence-bond or mesomeric approach, the preference for a homolytic C–P bond cleavage by $13.7 \text{ kcal mol}^{-1}$ (see above and Table 1) suggests a slightly dominating contribution of the purely covalent form (C–P). As emphasized above, the reversal of the relative covalent/dative character with respect to the amidiniophosphanes of type A is due to the electrostatic strain of the released $[(\text{NHC})\text{PPh}]^{2+}$ moiety that results from a heterolytic dissociation mode.

Electron-donating properties of diamidiniophosphanes. The FMOs of the phenylated phosphanes **9a–11a** and ethyl phosphinite **11b** (Scheme 5) were calculated at the PCM-B3PW91/6-31G** level (Figure 5). Upon replacement of the phenyl substituent of diamidiniophosphane **11a** by the ethoxy substituent in **11b**, the selected HOMOs, polarized on the lone pair of electrons on the P atom (quasi-degenerate with the HOMO for **9a** and **11b**), and the LUMO, polarized along the NHC–P bond, are shifted down to lower energy. As in the case of the model imidazoliophosphanes

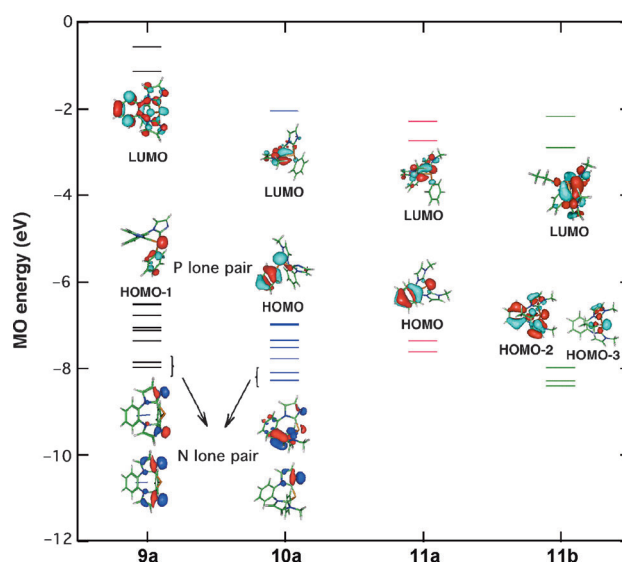


Figure 5. Selected near-frontier molecular orbitals of diimidazolophosphane derivatives in phenylphosphanes **9a–11a** and ethyl phosphinite **11b** series (Scheme 5). PCM-B3PW91/6-31G** level of calculation in the acetonitrile continuum ($\epsilon = 35.688$). For **9a**, **11a**, and **11b**, the selected orbitals with the highest contribution at the P atom and quasi-degenerate with the HOMO are displayed.

$[\text{NHC}-\text{PPh}_{2-a}(\text{OEt})_a]^+$ ($a = 0, 1, 2$; see above), both variations suggest a weaker P-donating character of **11b** with respect to **11a**. A similar trend is observed in the phenylated series going from the neutral diimidazolophosphane **9a** to the dicationic diimidazoliophosphane **11a** through the monocationic imidazo–imidazoliophosphane **10a** (Figure 5).

The actual donating character in the completed series of ligands ($L = \mathbf{9a, b, 10a, b}$, and $\mathbf{11a, b}$; Scheme 5) was evaluated by calculating the average IR C=O stretching frequencies in the corresponding $[\text{RhCl}(L)(\text{CO})_2]$ complexes (Table 3). This character decreases in the following order: **9a** < **9b** < **10a** < **10b** < **11a** < **11b**. Denoting the overall charge as q and the varying substituent on the P atom as R, the phosphane

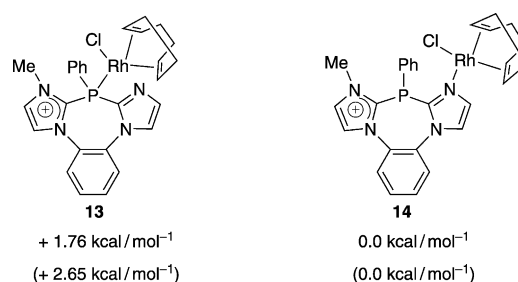
Table 3. Characteristics of $[\text{RhCl}(L)(\text{CO})_2]$ complexes calculated at the PCM-B3PW91/6-31G**/LANL2DZ*(Rh) level in the acetonitrile continuum ($\epsilon = 35.688$).

L ^[a]	q	R	Rh...P ^[b]	E_{diss} [kcal mol^{-1}] ^[c]	$\bar{\nu}_{\text{CO}}$ [cm^{-1}] ^[d]
9a	0	Ph	2.386	14.27	2053.6
9b	0	OEt	2.357	14.41	2056.9
10a	+1	Ph	2.377	6.32	2082.7
10b ^[e]	+1	OEt	2.344	6.75	2088.2
11a	+2	Ph	2.358	−2.67	2102.2
11b ^[e]	+2	OEt	2.352	−4.52	2102.5

[a] Variable ligands with formal charge q and monovalent P substituent R (Scheme 5). [b] Rh–P bond lengths in Å. [c] Zero-point corrected bond dissociation energies. [d] Average of the two IR C=O stretching frequencies calculated at the PBEPBE/6-31G**/LANL2DZ*(Rh) level in the gas phase. [e] Geometry optimization performed with looser convergence criteria than the default (calculation could not be achieved with default criteria).

and phosphinites subsequences **a** (R=Ph) and **b** (R=OEt) thus alternate perfectly in the main charge sequence $q=0, +1$, and $+2$ for **9**, **10**, and **11**, respectively, thus showing that the electron-withdrawing effect of substituting an ethoxy group (R=OEt) for a phenyl group (R=Ph) is much weaker ($0.3 < \tilde{\nu}_{\text{CO}} < 5.5 \text{ cm}^{-1}$) that the effect of adding a positive charge through a methylum cation ($14.3 < \tilde{\nu}_{\text{CO}} < 31.3 \text{ cm}^{-1}$). This outcome is in agreement with the previous observation in the $[\text{RhCl}(\text{L})_2(\text{CO})]$ series that the overall donating character of two imidazoliophosphane ligands is equivalent to that of two phosphite ligands (and not phosphinite ligands), namely, that the effect of one imidazolio P-substituent is equivalent to that of three alkoxy groups.^[5c] In the present $[\text{RhCl}(\text{L})(\text{CO})_2]$ series (Table 3), it is however noteworthy that the first N-methylation is twice as efficient at weakening the donating character of the ligand ($\Delta\tilde{\nu}_{\text{CO}} \approx 30 \text{ cm}^{-1}$ for **9**→**10**) than the second one ($\Delta\tilde{\nu}_{\text{CO}} \approx 15 \text{ cm}^{-1}$ for **10**→**11**). These results are in perfect agreement with the above FMO analysis (Figure 5).

Coordinating ability of diamidiniophosphanes. The weakening of the donation along the series **9a–11b** induces a vanishing coordinating ability to the Rh^{I} center. The corresponding dissociation energy E_{diss} decreases,^[22] and spontaneous dissociation is even predicted for the two last ligands **11a** and **11b** (Table 3). This finding is in line with the experimental results; that is, no $[\text{RhCl}(\text{cod})]$ complex could indeed be obtained from **11a**, in contrast to complexes **13–14** and **15**, which were readily formed from the phosphanes **9a** and **10a**, respectively (Scheme 6). From the monocationic phosphane **10a**, the P-coordinated complex **13** was however obtained in a 50:50 mixture with the N-coordinated complex **14** (Scheme 6). The FMOs of **9a** and **10a** (Figure 5) are similar and cannot account for the difference in the P-versus N-coordination selectivity. In both case, the HOMO is mainly polarized at the lone pair of electrons on the P atom, whereas molecular orbitals related to the lone pairs of electrons on the N atom are much lower in energy. Isomers **13** and **14** are calculated to be close in energy at the PCM-B3PW91/6-31G**/LANL2DZ*(Rh) level in the CH_2Cl_2 continuum ($\epsilon=8.93$), the N-coordinated isomer **14** is more stable than the P-coordinated isomer **13** by only 1.76 kcal mol⁻¹. These findings are therefore in favor of thermodynamic control of the coordination selectivity (Scheme 7).



Scheme 7. Relative stability of the isomeric complex ions **13** and **14** according to the zero-point corrected energies calculated at the PCM-B3PW91/6-31G**/LANL2DZ*(Rh) level in the dichloromethane continuum ($\epsilon=8.93$). Gibbs energies at 298.15 K are given in parenthesis.

Conclusion

In a comparative approach, the electron-poor ligands of the amidiniophosphane (**a**) and amidiniophosphinite (**b**) series of compounds can be classified according to the averaged $\tilde{\nu}_{\text{CO}}$ values in the corresponding $[\text{RhCl}(\text{L})(\text{CO})_2]$ complexes (Table 4). Substitution of a phenyl group by an imidazolio group was thus found to be more efficient at weakening the donating character of the ligand than substitution of a phenyl group by an ethoxy group. In spite of a slight structural difference due to the presence of the phenylene bridge between the imidazolyl moieties in **10a**, the relative ranks of the ethyl imidazoliophenylphosphinite ($\tilde{\nu}_{\text{CO}}=2072.7 \text{ cm}^{-1}$) and **10a** ($\tilde{\nu}_{\text{CO}}=2082.7 \text{ cm}^{-1}$) suggests that the electron-withdrawing effect on a P^{III} center of a neutral imidazolyl group is also superior to that of an ethoxy group. The scale also shows that the phosphane **11a** and phosphinite **11b** ($\tilde{\nu}_{\text{CO}} \approx 2102 \text{ cm}^{-1}$) are the least electron-donating potential ligands reported to date.^[23] Finally, the monocationic phosphane **10a** ($\tilde{\nu}_{\text{CO}} \approx 2082.7 \text{ cm}^{-1}$) appears as the most electron-poor ligand of the series that preserve actual P-coordinating properties toward a Rh^{I} center (in complex **13**). The coordinating properties of the extreme ligands **10a**, **11a**, and **11b** toward stronger Lewis acidic centers certainly deserve further investigation that could open more applied perspectives, in particular in catalysis.

Table 4. Scale of the electron-donating properties of potential ligands L based on the average IR C=O stretching frequencies (in cm^{-1}) in the corresponding $[\text{RhCl}(\text{L})(\text{CO})_2]$ complexes (calculated at the PBEPBE/6-31G**/LANL2DZ*(Rh) level in the gas phase).^[a]

L	$\text{P}(\text{OEt})_3$	$\text{P}(\text{OPh})_3$							
			3a model	10a	11a	11b			
$\tilde{\nu}_{\text{CO}}$	2058.5	2060.4	2071.6	2072.7	2075.9	2077.9	2082.7	2102.2	2102.5

[a] The actual coordinating limit of electron-poor ligands is between **10a** and **11a**.

Experimental Section

Computational details: Geometries were fully optimized at the PCM-B3PW91/6-31G**/LANL2DZ*(Rh) level of calculation using Gaussian09.^[24] LANL2DZ*(Rh) means that f-polarization functions derived by Ehlers et al.^[25] for Rh have been added to the LANL2DZ(Rh) basis set. Vibrational analysis was performed at the same level as the geometry optimization. Solvent effects were included using the polarizable continuum model (PCM) implemented in Gaussian09 either for acetonitrile ($\epsilon = 35.688$) or dichloromethane ($\epsilon = 8.93$). Gibbs energies were calculated at 298.15 K. IR C=O stretching frequencies were calculated in the gas phase at the PBEPBE/6-31G**/LANL2DZ*(Rh) level. Molecular orbitals were plotted using the GABEDIT program.^[26]

Crystal structure determination of 9a, 11a, 14, and 15: X-ray diffraction data for the crystals were collected at low temperature on a Bruker Apex2, an Oxford Diffraction Xcalibur, or an Oxford Diffraction Gemini diffractometer using a graphite-monochromated MoK α radiation source (9a, 11a, and 15: $\lambda = 0.71073$ Å) or CuK α radiation source (14: $\lambda = 1.54180$ Å). Multiscan absorption corrections were applied. The structures were solved by direct methods using SIR92^[27] or SUPERFLIP^[28] and refined by means of least-square procedures with the programs of the PC version of CRYSTALS.^[29] Atomic scattering factors were taken from the International tables for X-ray crystallography.^[30] All non-hydrogen atoms were refined anisotropically. Hydrogen atoms were refined with riding constraints.

9a: C₁₈H₁₃N₄P, $M_r = 316.30$ g mol⁻¹, monoclinic, $a = 12.9720(5)$, $b = 12.0665(4)$, $c = 10.0953(4)$ Å, $\beta = 107.309(4)^\circ$, $V = 1508.62(10)$ Å³, $T = 180$ K, space group Cc , $Z = 4$, $\mu(\text{MoK}\alpha) = 0.187$ mm⁻¹, 7963 reflections measured, 3888 unique ($R_{\text{int}} = 0.017$), 209 parameters, refinement on F , 3557 reflections used in the calculations [$I > 3\sigma(I)$], $R1 = 0.0265$, $wR2 = 0.0314$.

11a: C₂₀H₁₉N₄P, 2(CF₃O₃S), C₂H₅N, $M_r = 685.56$ g mol⁻¹, orthorhombic, $a = 10.3919(6)$, $b = 23.7534(14)$, $c = 24.5833(14)$ Å, $V = 6068.2(6)$ Å³, $T = 180$ K, space group $Pbca$, $Z = 8$, $\mu(\text{MoK}\alpha) = 0.312$ mm⁻¹, 14 1761 reflections measured, 8925 unique ($R_{\text{int}} = 0.044$), 397 parameters, refinement on F^2 , 5441 reflections used in the calculations [$I > 3\sigma(I)$], $R1 = 0.0555$, $wR2 = 0.1435$.

14: C₂₇H₂₈ClN₄PRh, CF₃O₃S, CH₂Cl₂, $M_r = 811.88$ g mol⁻¹, triclinic, $a = 9.5244(4)$, $b = 13.4771(8)$, $c = 14.1632(7)$ Å, $\alpha = 64.578(5)$, $\beta = 85.402(4)$, $\gamma = 78.637(4)^\circ$, $V = 1609.77(16)$ Å³, $T = 100$ K, space group $P\bar{1}$, $Z = 2$, $\mu(\text{CuK}\alpha) = 8.150$ mm⁻¹, 19 499 reflections measured, 4842 unique ($R_{\text{int}} = 0.043$), 406 parameters, refinement on F , 4367 reflections used in the calculations [$I > 3\sigma(I)$], $R1 = 0.0245$, $wR2 = 0.0254$.

15: C₂₆H₂₅ClN₄PRh, $M_r = 562.84$ g mol⁻¹, triclinic, $a = 8.6872(3)$, $b = 9.6723(3)$, $c = 15.2200(5)$ Å, $\alpha = 108.511(3)$, $\beta = 94.614(3)$, $\gamma = 104.558(3)^\circ$, $V = 1155.73(7)$ Å³, $T = 180$ K, space group $P\bar{1}$, $Z = 2$, $\mu(\text{MoK}\alpha) = 0.947$ mm⁻¹, 50 571 reflections measured, 5882 unique ($R_{\text{int}} = 0.066$), 298 parameters, refinement on F , 4694 reflections used in the calculations [$I > 3\sigma(I)$], $R1 = 0.0306$, $wR2 = 0.0330$.

Acknowledgements

The authors thank the Ministère de l'Enseignement Supérieur de la Recherche et de la Technologie and the Université Paul-Sabatier, the Centre National de la Recherche Scientifique and the ANR program (ANR-08-JCJC-0137-01) for the doctoral fellowship of C.M. The theoretical studies were performed using HPC resources from CALMIP (Grant 2010 and 2011 [0851]) and from GENCI-[CINES/IDRIS] (Grant 2010 and 2011 [085008]).

[1] According to L. C. Allen, electronegativity is the "third dimension" of the Periodic Table; a) L. C. Allen, *J. Am. Chem. Soc.* **1989**, *111*, 9003; b) X. Sun, *The Chemical Educator* **2000**, *5*, 54.

- [2] a) K. B. Dillon, F. Mathey, J. F. Nixon in *Phosphorus: The Carbon Copy*, Wiley, Chichester, **1998**; b) R. Zurawinski, B. Donnadiou, M. Mikolajczyk, R. Chauvin, *J. Organomet. Chem.* **2004**, *689*, 380.
- [3] *Multiple Bonds and Low Coordination in Phosphorus Chemistry* (Eds.: M. Regitz, O. J. Scherer), Thieme, Stuttgart, **1990**.
- [4] a) J. F. Harrison, *J. Am. Chem. Soc.* **1981**, *103*, 7406; b) D. Gudat, *Eur. J. Inorg. Chem.* **1998**, 1087; c) D. Gudat, A. Haghverdi, H. Hupfer, M. Nieger, *Chem. Eur. J.* **2000**, *6*, 3414; d) C. A. Caputo, M. C. Jennings, H. M. Tuononen, N. D. Jones, *Organometallics* **2009**, *28*, 990; e) D. Gudat, *Acc. Chem. Res.* **2010**, *43*, 1307.
- [5] a) N. Kuhn, J. Fahl, D. Bläser, R. Boese, *Z. Anorg. Allg. Chem.* **1999**, *625*, 729; b) M. Azouri, J. Andrieu, M. Picquet, P. Richard, B. Hanquet, I. Tkatchenko, *Eur. J. Inorg. Chem.* **2007**, 4877; c) Y. Canac, N. Debono, L. Vendier, R. Chauvin, *Inorg. Chem.* **2009**, *48*, 5562; d) Y. Canac, N. Debono, C. Lepetit, C. Duhayon, R. Chauvin, *Inorg. Chem.* **2011**, *50*, 10810; e) J. J. Weigand, K. O. Feldmann, F. D. Henne, *J. Am. Chem. Soc.* **2010**, *132*, 16321; f) J. Petuskova, H. Bruns, M. Alcarazo, *Angew. Chem.* **2011**, *123*, 3883; *Angew. Chem. Int. Ed.* **2011**, *50*, 3799.
- [6] Although a dative bond can be considered as intermediate between a pure (homopolar) covalent bond and a pure ionic bond (in the valence bond approach), thus varying with polarity so that very polar bonds are definitely nondative; for example, in the gas phase, the heterolytic bond dissociation energy (BDE) of the highly polar ⁺H–F^{-q} bond ($\mu = 1.826$ D, $q = 0.225$ e) is two times greater (1548 kJ mol⁻¹) than the corresponding homolytic BDE (569 kJ mol⁻¹); this homolytic dissociation preference for such a neutral motif is actually due to the electrostatic cost of the H⁺...F⁻ charge separation in the heterolytic mode; in the case of ionic motifs, such as amidiniophosphanes, the electrostatic cost is cancelled, thus possibly conferring a dative nature to bonds between atoms of similar electronegativities (even if the bond is weakly polar with respect to the bond center when the charge is uniformly delocalized between the two atoms in the ground state); for relevant discussions, see: a) R. S. Mulliken, W. B. Person, *Ann. Pharm. Belg. Ann. Rev. Phys. Chem.* **1962**, *13*, 107; b) R. S. Mulliken, *J. Am. Chem. Soc.* **1952**, *74*, 811; c) A. Haaland, *Angew. Chem.* **1989**, *101*, 1017; *Angew. Chem. Int. Ed. Engl.* **1989**, *28*, 992; d) V. I. Minkin, *Pure Appl. Chem.* **1999**, *71*, 1919; the observable global dative character of a bond could however be analyzed in more detail by "subtracting" the electrostatic contribution from the crude BDE values, which could be achieved by natural bond order (NBO) analysis (e.g., through the Wiberg indexes) or by topological analysis of the electron density (e.g., through the sign of the Laplacian at the bond critical point) or of the electron-localization function (e.g., through the position of the attractor in the bond-valence basin).
- [7] a) B. D. Ellis, P. J. Ragogna, C. L. B. Macdonald, *Inorg. Chem.* **2004**, *43*, 7857; b) N. Debono, Y. Canac, C. Duhayon, R. Chauvin, *Eur. J. Inorg. Chem.* **2008**, 2991.
- [8] a) I. Abdellah, C. Lepetit, Y. Canac, C. Duhayon, R. Chauvin, *Chem. Eur. J.* **2010**, *16*, 13095; b) I. Abdellah, M. Boggio-Pasqua, Y. Canac, C. Lepetit, C. Duhayon, R. Chauvin, *Chem. Eur. J.* **2011**, *17*, 5110; c) Y. Canac, C. Maaliki, I. Abdellah, R. Chauvin, *New J. Chem.* **2012**, *36*, 1727.
- [9] a) A. H. Cowley, R. A. Kemp, *Chem. Rev.* **1985**, *85*, 367; b) M. Sanchez, M. R. Mazières, L. Lamandé, R. Wolf, "Phosphenium cations" in *Multiple Bonds and Low Coordination In Phosphorus Chemistry*, (Eds.: M. Regitz, O. J. Scherer), Thieme, Stuttgart, Germany, **1990**, p129–148; c) D. Gudat, *Coord. Chem. Rev.* **1997**, *163*, 71.
- [10] N. J. Hardman, M. B. Abrams, M. A. Pribisko, T. M. Gilbert, R. L. Martin, G. J. Kubas, R. T. Baker, *Angew. Chem.* **2004**, *116*, 1989; *Angew. Chem. Int. Ed.* **2004**, *43*, 1955.
- [11] a) J. J. Brunet, R. Chauvin, G. Commenges, B. Donnadiou, P. Leglaye, *Organometallics* **1996**, *15*, 1752; b) N. Kuhn, M. Göhner, M. Steimann, *Z. Anorg. Allg. Chem.* **2002**, *628*, 896; c) P. Leglaye, B. Donnadiou, J. J. Brunet, R. Chauvin, *Tetrahedron Lett.* **1998**, *39*, 9179; d) L. Viau, R. Chauvin, *J. Organomet. Chem.* **2002**, *654*, 180; e) V. Cadierno, J. Francos, J. Gimeno, *Chem. Eur. J.* **2008**, *14*, 6601;

- f) D. J. M. Snelders, G. v. Koten, R. J. M. Klein Gebbink, *Chem. Eur. J.* **2011**, *17*, 42.
- [12] M. Azouri, J. Andrieu, M. Picquet, H. Cattey, *Inorg. Chem.* **2009**, *48*, 1236.
- [13] J. Petuskova, M. Patil, S. Holle, C. W. Lehmann, W. Thiel, M. Alcarazo, *J. Am. Chem. Soc.* **2011**, *133*, 20758.
- [14] a) Y. Canac, C. Duhayon, R. Chauvin, *Angew. Chem.* **2007**, *119*, 6429; *Angew. Chem. Int. Ed.* **2007**, *46*, 6313; b) Y. Canac, C. Lepetit, M. Abdalilah, C. Duhayon, R. Chauvin, *J. Am. Chem. Soc.* **2008**, *130*, 8406.
- [15] A. B. Salah, D. Zargarian, *Dalton Trans.* **2011**, *40*, 8977.
- [16] S. P. Nolan, US Patent Application Serial No 10/653,688 (September 2, **2003**).
- [17] Y. H. So, *Macromolecules* **1992**, *25*, 516.
- [18] CCDC-858972 (**9a**), CCDC-858973 (**11a**), CCDC-858974 (**14**), and CCDC-863842 (**15**) contain the supplementary crystallographic data for this paper. These data can be obtained free of charge from The Cambridge Crystallographic Data Centre via www.ccdc.cam.ac.uk/data_request/cif.
- [19] A. R. Chianese, X. Li, M. C. Janzen, J. W. Faller, R. H. Crabtree, *Organometallics* **2003**, *22*, 1663.
- [20] The given values correspond to the most stable calculated conformers.
- [21] G. Canepa, C. D. Brandt, H. Werner, *Organometallics* **2004**, *23*, 1140.
- [22] It is noteworthy that the calculated Rh–P bond lengths are not consistently correlated with E_{diss} ; secondary conformational and/or electronic effects might be sought for.
- [23] D. Martin, D. Moraleda, T. Achard, L. Giordano, G. Buono, *Chem. Eur. J.* **2011**, *17*, 12729.
- [24] Gaussian 09, Revision A.1, M. J. Frisch, G. W. Trucks, H. B. Schlegel, G. E. Scuseria, M. A. Robb, J. R. Cheeseman, G. Scalmani, V. Barone, B. Mennucci, G. A. Petersson, H. Nakatsuji, M. Caricato, X. Li, H. P. Hratchian, A. F. Izmaylov, J. Bloino, G. Zheng, J. L. Sonnenberg, M. Hada, M. Ehara, K. Toyota, R. Fukuda, J. Hasegawa, M. Ishida, T. Nakajima, Y. Honda, O. Kitao, H. Nakai, T. Vreven, Jr., J. A. Montgomery, J. E. Peralta, F. Ogliaro, M. Bearpark, J. J. Heyd, E. Brothers, K. N. Kudin, V. N. Staroverov, R. Kobayashi, J. Normand, K. Raghavachari, A. Rendell, J. C. Burant, S. S. Iyengar, J. Tomasi, M. Cossi, N. Rega, N. J. Millam, M. Klene, J. E. Knox, J. B. Cross, V. Bakken, C. Adamo, J. Jaramillo, R. Gomperts, R. E. Stratmann, O. Yazyev, A. J. Austin, R. Cammi, C. Pomelli, J. W. Ochterski, R. L. Martin, K. Morokuma, V. G. Zakrzewski, G. A. Voth, P. Salvador, J. J. Dannenberg, S. Dapprich, A. D. Daniels, O. Farkas, J. B. Foresman, J. V. Ortiz, J. Cioslowski and D. J. Fox, Gaussian, Inc., Wallingford CT, **2009**.
- [25] A. W. Ehlers, M. Böhme, S. Dapprich, A. Gobbi, A. Höllwarth, V. Jonas, K. F. Köhler, R. Stegmann, A. Veldkamp and G. Frenking, *Chem. Phys. Lett.* **1993**, *208*, 111.
- [26] <http://sites.google.com/site/allouche/HOME/gabedit>.
- [27] A. Altomare, G. Cascarano, C. Giacovazzo, A. Guagliardi, M. C. Burla, G. Polidori, M. Camalli, *J. Appl. Crystallogr.* **1994**, *27*, 435.
- [28] L. Palatinus, G. Chapuis, *J. Appl. Crystallogr.* **2007**, *40*, 786.
- [29] P. W. Betteridge, J. R. Carruthers, R. I. Cooper, K. Prout, D. J. Watkin, *J. Appl. Crystallogr.* **2003**, *36*, 1487.
- [30] *International Tables for X-ray Crystallography, Vol. IV*, Kynoch Press, Birmingham, England, **1974**.

Received: December 24, 2011
Revised: February 27, 2012
Published online: May 31, 2012